Protist, Vol. 163, 188–203, March 2012
http://www.elsevier.de/protis
Published online date 3 August 2011

Protist

ORIGINAL PAPER

Plastidic Phosphoglycerate Kinase from *Phaeodactylum tricornutum*: On the Critical Role of Cysteine Residues for the Enzyme Function

María Belén Bosco, Mabel Cristina Aleanzi, and Alberto Álvaro Iglesias[1]

Laboratorio de Enzimología Molecular, Instituto de Agrobiotecnología del Litoral (IAL, CONICET-UNL), Facultad de Bioquímica y Ciencias Biológicas, Paraje "El Pozo", CC 242, S3000ZAA Santa Fe, Argentina

Submitted January 21, 2011; Accepted June 23, 2011
Monitoring Editor: Saul Purton

Chloroplastidic phosphoglycerate kinase (PGKase) plays a key role in photosynthetic organisms, catalyzing a key step in the Calvin cycle. We performed the molecular cloning of the gene encoding chloroplastidic PGKase-1 in the diatom *Phaeodactylum tricornutum*. The recombinant enzyme was expressed in *Escherichia coli*, purified and characterized. Afterward, it showed similar kinetic properties than the enzyme studied from other organisms, although the diatom enzyme displayed distinctive responses to sulfhydryl reagents. The activity of the enzyme was found to be dependent on the redox status in the environment, determined by different compounds, including some of physiological function. Treatment with oxidant agents, such as diamide, hydrogen peroxide, glutathione and sodium nitroprusside resulted in enzyme inhibition. Recovery of activity was possible by subsequent incubation with reducing reagents such as dithiothreitol and thioredoxins (from *E. coli* and *P. tricornutum*). We determined two midpoint potentials of different regulatory redox centers, both values indicating that PGKase-1 might be sensitive to changes in the intracellular redox environment. The role of all the six Cys residues found in the diatom enzyme was analyzed by molecular modeling and site-directed mutagenesis. Results suggest key regulatory properties for *P. tricornutum* PGKase-1, which could be relevant for the functioning of photosynthetic carbon metabolism in diatoms.

Key words: *Phaeodactylum tricornutum*; phosphoglycerate kinase; redox regulation.

Introduction

Diatoms are unicellular photosynthetic eukaryotes that contribute to about one quarter of global primary productivity (Bowler et al. 2008). Despite their importance, very little is known about the biology of these microorganisms at the molecular level. Diatom chloroplasts evolved by secondary endocytobiosis, via uptake of an eukaryotic algae into another eukaryotic heterotrophic host cell, with its subsequent evolutionary reduction to one organelle (Scala et al. 2002). In consequence, diatom chloroplasts differ from those in plants; as, for example, the former are surrounded by four membranes and they possess an incomplete oxidative pentose phosphate pathway (OPP) (Gruber et al. 2009). *Phaeodactylum tricornutum* is a representative member that has been widely utilized as a model system for studies on diatoms. The recent elucidation of the entire genome of *P. tricornutum* (Bowler et al. 2008) proved mandatory to advance

[1]Corresponding author; fax +54-342-457 5209x217
e-mail iglesias@fbcb.unl.edu.ar (A.Á. Iglesias).

doi:10.1016/j.protis.2011.07.001

in the molecular cloning of genes, and the production and characterization of recombinant enzymes to establish the occurrence and functionality of metabolic scenarios in the organism.

Phosphoglycerate kinase (EC 2.7.2.3, PGKase) catalyzes the ATP-dependent phosphorylation of 3-phospho-glycerate (3PGA) to 1,3-bis-phospho-glycerate (1,3-bisPGA), in a reversible reaction requiring Mg^{2+} as essential cofactor. The enzyme is found in all kingdoms, with the occurrence of forms localizing in different intracellular compartments (Joao and Williams 1993). In photosynthetic organisms, the chloroplastidic enzyme plays a key role, catalyzing the step following carbon fixation by the Calvin cycle (Joao and Williams 1993). PGKase is a monomeric enzyme having two domains, with a deep cleft between them (Banks et al. 1979). Binding of 3PGA occurs at the N-terminus, while ATP-Mg binds to the C-terminal domain of the enzyme. Conformational changes bringing the two domains in close proximity take place during catalysis and generate the closed form of the protein that allows the transfer of the phosphate group. The PGKase sequence remained highly conserved during evolution (Joao and Williams 1993), although the number of Cys residues is significantly different between species. Yeast PGKase has one Cys and shows no loss of activity when incubated with thiol-modifying agents (Krietsch and Bucher 1970; Markland et al. 1975); whereas the mammalian enzyme has seven Cys residues and is inactivated by treatment with DTNB or alkylating reagents (Cserpan and Vas 1983; Dekany and Vas 1984; Huskins et al. 1982). It has been proposed that two Cys residues, adjacent to the C-terminus of the primary structure, are responsible for this phenomenon, later they were referred to “fast-reacting” (Cserpan and Vas 1983; Minard et al. 1989).

P. tricornutum contains three sequences coding for PGKase in its genome (Bowler et al. 2008). The enzymes localize either in the cytosol (*Ptr*PGKase-51125), mitochondria (*Ptr*PGKase-2) or chloroplast (*Ptr*PGKase-1) (Liaud et al. 2000). We performed the molecular cloning of the gene to heterologously express, purify and characterize the chloroplastidic PGKase-1 of the diatom. Kinetic parameters and the reaction mechanism determined for the recombinant enzyme were similar to those described previously for other PGKases. Interestingly, we found distinctive responses of *Ptr*PGKase-1 to thiol modifying reagents. We determined that the activity of the enzyme is dependent on the redox status in the environment established by physiological compounds. To the best of our knowledge, this is the first study advancing the characterization of a PGKase from diatoms and determining the occurrence of redox regulation mechanisms in these microorganisms.

Results

Molecular Cloning, Expression and Purification of *Ptr*PGKase-1

A comparison of PGKase amino acid sequences from different sources indicates a high degree of conservation at the level of primary structure (Fig. 1), especially with respect to functional residues. Thus, the alignment of amino acid sequences of 11 PGKases shows 71 residues totally conserved and a larger number of conservative substitutions, leading to a 14% identity and 64% similarity in the whole comparison (Fig. 1). On this basis, it has been proposed that the tertiary structure and the active-site regions of PGKases are conserved (Fifis and Scopes 1978). *P. tricornutum* contains three sequences coding for PGKase in its genome, and it is deducted that the enzymes localize either in the cytosol (*Ptr*PGKase-51125), mitochondria (*Ptr*PGKase-2) or chloroplast (*Ptr*PGKase-1) (Liaud et al. 2000). The gene encoding chloroplastidic PGKase-1 (accession number AF108451, protein ID 29157) in the microorganism contains a bipartite signal/transit peptide of 42 amino acids (Fig. 1), necessary for precursor-protein import across the four membranes that surround the diatom plastids. The previously predicted length and processing site of this peptide (Liaud et al. 2000) were used in order to clone and heterologously express the plastidic enzyme in *E. coli*.

We cloned the AF108451 gene without the bipartite transit peptide in the expression vector pET-19b to obtain the mature *Ptr*PGKase-1, with the addition of a His_{10}-tag at the N-terminus to simplify protein purification. Competent *E. coli* Rosetta (DE3) cells were transformed with the resultant construct and the expressed enzyme was highly purified by IMAC (Fig. 2). Studies performed using gel filtration chromatography showed that *Ptr*PGKase-1 was a monomer of 45 kDa. The purified enzyme reached a specific activity of 47.5 units mg^{-1} and displayed the kinetic parameters shown in Table 1. Values of V_M, $S_{0,5}$ and n_H obtained for the diatom enzyme are quite similar to those reported for PGKases from bacteria (Nojima et al. 1979; Pawluk et al. 1986), cyanobacteria (Kuntz and Krietsch 1982), yeasts (Krietsch and Bucher 1970; Kuntz and

Figure 1. Amino acids sequence alignment of PGKases from different sources. *Ptr*, *Phaeodactylum tricornutum*; *Tps*, *Thalassiosira pseudonana* (diatom); *Sol*, *Spinacea oleracea* (spinach); *Cre*, *Chlamydomonas reinhardtii*; *Hsa*, *Homo sapiens*; *Ssc*, *Sus scrofa* (pig); *Sce*, *Saccharomyces cerevisiae*; *Tca*, *Thermus caldophilus*; *Eco*, *E. coli*. *Cre*, *Sol*, *Tps* and *PtrP*-1 possess chloroplastidic signal peptides, the *Phaeodactylum* one is coloured in pink. The number 1 residue is the first amino acid in the expressed *Ptr*PGKase-1 (see text). *Ptr*P-2 and *Ptr*P-51125 are targeted to the mitochondria and cytosol, respectively. Residues alignment colour key: non-similar (black letter), conservative (shaded cyan), block of similar (shaded green) and weakly similar (green letter). The black dots localize Cys residues under study in the present work. (For interpretation of the references to color in this figure legend, the reader is referred to the web version of the article.)

Krietsch 1982), protozoa (Zomer et al. 1998), mammals (Fritz and White 1974; Krietsch and Bucher 1970; Krietsch et al. 1980) and plants PGKases (Kuntz and Krietsch 1982). As for other PGKases (Larsson-Raznikiewicz and Arvidsson 1971), a random-binding order mechanism, in which the binding of one substrate does not affect the binding of the other was observed for *Ptr*PGKase-1 (data not shown).

Table 1. Kinetic parameters of purified *Ptr*PGKase-1.

Substrate	$S_{0.5}$ (mM)	n_H	V_M (U mg^{-1})
3PGA	1.55	0.9	47.5
ATP	0.89	0.6	
Mg^{2+}	0.36	0.9	

Redox Properties of *Ptr*PGKase-1

We observed that *Ptr*PGKase-1 lost its activity when stored in the absence of a reducing agent. In fact, although it lacks the conserved adjacent Cys residues in the C-terminal domain, whose oxidation was postulated to be responsible for inactivation of the mammalian enzyme (Huskins et al. 1982), we found that *Ptr*PGKase-1 was inhibited by the non-physiological thiol-modifying agent diamide. As shown in Figure 3, the enzyme inactivation exhibited pseudo-first-order kinetics when the oxidant agent was present in a molar excess of 10- to 10,000-fold. Also, inactivation followed a two-step mechanism, as the plot of k'_{obs} as a function of inhibitor concentration showed saturation, reaching a plateau at high values of oxidant concentration (Fig. 3, inset).

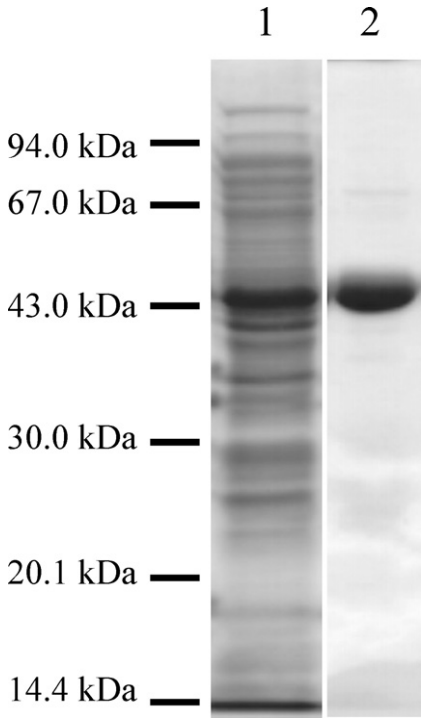

Figure 2. Reducing SDS-PAGE (12.5%) of IMAC purification of recombinant *Ptr*PGKase-1. Lanes: 1, crude extract; 2, enzyme recovered after IMAC. Molecular mass markers: phosphorylase b (94.0 kDa), BSA (67.0 kDa), ovalbumin (43.0 kDa), carbonic anhydrase (30.0 kDa), trypsin inhibitor (20.1 kDa), α-lactalbumin (14.4 kDa).

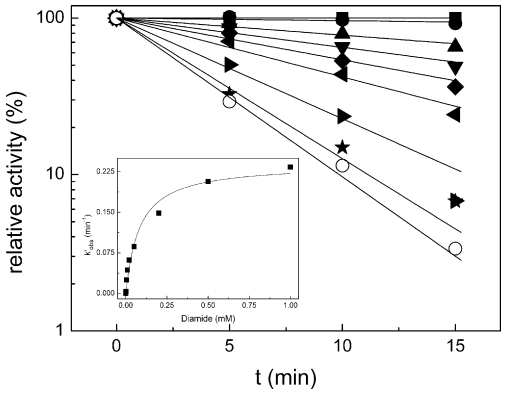

Figure 3. Kinetic characterization of wild type *Ptr*PGKase-1 inactivation by diamide. 0.1 μM purified enzyme was incubated, as specified under Methods, at 25 °C with various concentrations (in mM) of diamide: 0 (■), 0.001 (●), 0.005 (▲), 0.01 (▼), 0.02 (♦), 0.05 (◄), 0.2 (►), 0.5 (★) and 1 (◯). For incubation condition, percentage of residual enzymatic activity (relative activity) was measured at variable incubation times. Inset: plot of pseudo-first-order reaction rate constant (k'_{obs}) vs. diamide concentration.

As diamide is not a cellular reagent, we investigated if *Ptr*PGKase-1 was inactivated by physiological oxidants such as H_2O_2, GSSG and NPS (nitric oxide donor). Effectively, these compounds inhibited the enzyme following the same two-step mechanism observed for diamide. As shown in Table 2, inhibitors exhibited different effec-

Table 2. Kinetic constants for the oxidation of wild type and mutants *Ptr*PGKase-1. Values were calculated form pseudo-first-order kinetics as specified under Methods.

Oxidant	Wild type	C21S	C58S	C77S	C95S	C214S	C312S
DIAMIDE							
k′(min)	0.24	0.17	1.20	0.95	0.68	0.18	0.27
K_I (μM)	82.0	52.0	10.3	7.11	6.05	144	50.0
k″ (M^{-1} s^{-1})	49.0	55.0	1940	2220	1860	21.0	89.0
H_2O_2							
k′ (min)	0.16	0.10	1.22	0.40	0.25	0.08	0.15
K_I (μM)	1500	1790	3270	1280	518	1100	2220
k″ (M^{-1} s^{-1})	1.77	0.93	6.22	5.15	8.08	1.18	1.10
NPS							
k′ (min)	0.08						
K_I (μM)	437						
k″ (M^{-1} s^{-1})	2.90						
GSSG							
k′ (min)	0.01						
K_I (μM)	480						
k″ (M^{-1} s^{-1})	0.30						

tiveness, with diamide being the best oxidant and GSSG exhibiting the lowest value of k″. Differences in k″ values for the inhibitors were due to changes in the apparent affinity of the enzyme for each oxidant (K_I) rather than to modifications in k′, except for NPS and GSSG that showed similar K_I.

*Ptr*PGKase-1 contains six Cys residues, at positions 21, 58, 77, 95, 214 and 312. The first four residues are located in the N-terminal and the last two in the C-terminal domain. Using a constructed homology model of the diatom enzyme in the open conformation, we determined that distances between these Cys residues are within 6-15 Å (Supplementary Fig. S1 and Table S1), with the closer distances found for pairs: 58-95, 21-58, and 214-312. Although these proximities between Cys residues are not optimal to undergo disulphide links, it is worth mentioning that the positioning of the Cys residues in the model has relatively low accuracy, since templates have no conserved Cys in those positions. Also, rearrangement of side chains could bring the sulfhydryl groups to distances closer and more suitable to form disulphide bridges.

To probe the role of these residues in regulation of the enzyme, single mutants of all six Cys were constructed: C21S, C58S, C77S, C95S, C214S and C312S. His_{10}-tag mutant enzymes were purified to homogeneity, following the same procedure as for the wild type *Ptr*PGKase-1. All mutant enzymes exhibited similar V_M than the wild type proteins, although mutants C21S, C58S, C77S and C95S displayed a slightly lower affinity for 3PGA (data not shown). None of the single mutant enzymes exhibited insensitivity to the oxidants but, as a whole, all of them showed the same pseudo-first-order inactivation kinetics as the wild type *Ptr*PGKase-1. Results suggest that enzyme inactivation would not be a consequence of the oxidation of a single Cys residue in PGKase. From Table 2, it can be seen that C21S, C214S and C312S mutants behaved in a similar way as the wild type enzyme respect to the oxidants, indicating that none of the Cys residue mutated alone seemed to be responsible for the oxidative enzyme inactivation. Remarkably, C58S, C77S and C95S were notably more sensitive to diamide oxidation than the wild type enzyme, exhibiting higher affinity for the inhibitor (Table 2). This phenomenon was still evident with hydrogen peroxide inactivation, but in lower degree extent. These results suggest that these three Cys residues would be important in redox inactivation.

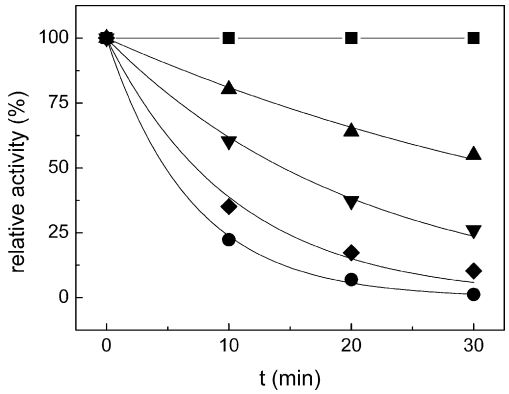

Figure 4. Protection afforded by substrates against inactivation of *Ptr*PGKase-1 by oxidation with 0.1 mM diamide. The enzyme (0.1 μM) was preincubated at 25 °C in the assay medium in the presence of different substrates: none (●), 5 mM 3PGA (▲), 5 mM ATP (▼), 5 mM ATP and 5 mM $MgCl_2$ (♦). Control without oxidant was included (■).

Substrate protection against diamide oxidation was also assayed. As seen in Figure 4, protection was mainly achieved by 3PGA and ATP, with a minor effect observed for ATP-Mg. The protective effect afforded by 3PGA and ATP was dependent on the concentration of each substrate in the modification medium, from which it was possible to estimate the respective K_d value for the binding, using the approach developed by Mildvan and Leigh (Mildvan and Leigh 1964). Since Cys-21, Cys-58, Cys-77 and Cys-95 are close to the 3PGA binding site, protection exerted by this substrate was not surprising (K_d^{3PGA} = 0.97 mM). With regard to ATP protection, we observed that the Mg-free nucleotide was the true effector (K_d^{ATP} = 1.7 mM) rather than the complex ATP-Mg. In fact, protection observed with ATP-Mg was only due to a secondary effect of the portion of free ATP present in the equilibrium established in the formation of the complex (data not shown). NMR studies have revealed a second binding site for Mg-free ATP (and for other anions such as sulphate), which overlaps with at least a part of the 3PGA binding site that localizes in a positively charged region of the N-terminus called 'basic patch' (Joao and Williams 1993). Residues Cys-214 and Cys-312 are located near the C-terminus but relatively far from the site where ATP-Mg binds. It is suggested that both, free ATP and 3PGA protection could be a consequence of steric effects that hide Cys residues near the 3PGA binding site, and which are responsible for the loss of enzymatic activity. Free Mg^{2+} did not protect *Ptr*PGKase-1 from oxidation.

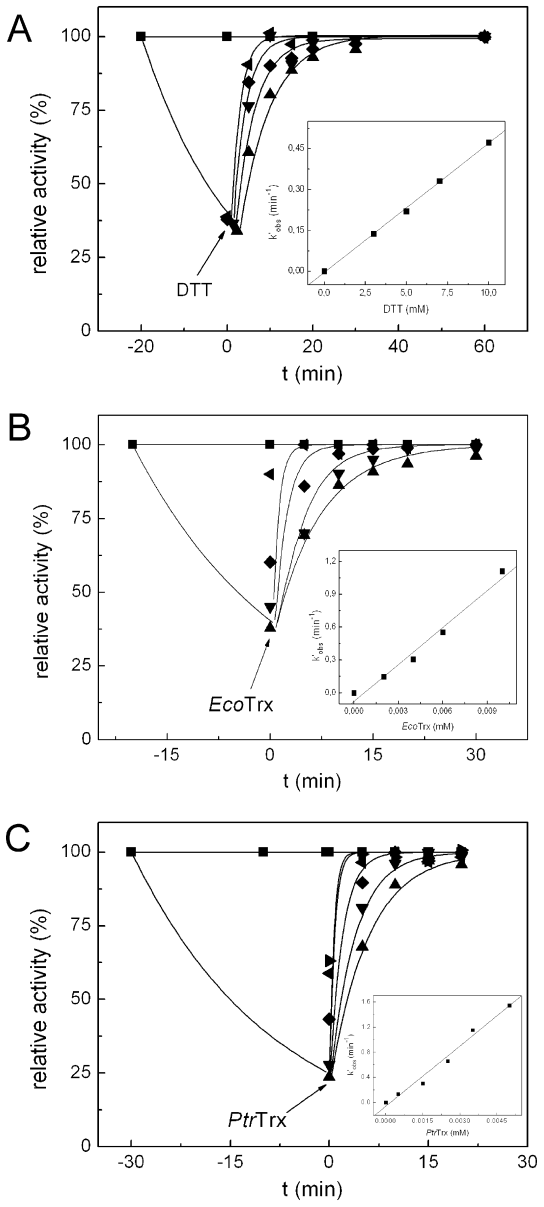

Figure 5. Kinetic characterization of wild type *Ptr*PGKase-1 activation by reducing agents. 0.1 μM *Ptr*PGKase-1 was oxidized with 0.5 mM H_2O_2 during 20 to 30 min at 25 °C. Afterward (zero time) the oxidized enzyme was incubated with various concentrations of reducing agents and percentage of enzymatic activity (relative activity) was measured at each indicated time. Control without oxidant was included (■). (**A**) DTT reduction: oxidized enzyme plus DTT: 3 mM (▲), 5 mM (▼), 7 mM (♦) and 10 mM (◄); (**B**) *Eco*Trx reduction: oxidized enzyme plus *Eco*Trx: 2 μM (▲), 4 μM (▼), 6 μM (♦) and 10 μM (◄); (**C**) *Ptr*Trx reduction: oxidized enzyme plus *Ptr*Trx: 0.5 μM (▲), 1.5 μM (▼), 2.5 μM (♦), 3.5 μM (◄) and 5 μM (►). Insets: plots of pseudo-first-order reaction rate constant (k'_{obs}) vs. reducing agent concentration.

Table 3. Reduction kinetic constants for wild type *Ptr*PGKase-1, calculated as explained in Methods.

Oxidant agent	Reducing agent	k″ ($M^{-1}\,s^{-1}$)
Diamide	DTT	0.188
	*Eco*Trx	2345
	*Ptr*Trx	1163
H_2O_2	DTT	0.790
	*Eco*Trx	1873
	*Ptr*Trx	5328
NPS	DTT	n.d.[a]
	*Eco*Trx	2034
	*Ptr*Trx	n.d.

[a]n.d., not determined.

Physiological redox regulation of a protein not only involves its oxidation but also the reversion of the process by reductant agents. We tested chemical (DTT) and biological compounds [*E. coli* Trx (*Eco*Trx) and *P. tricornutum* periplastidic Trx-h2 (*Ptr*Trx, protein ID 48539)] as reducing agents of *Ptr*PGKase-1 previously oxidized with diamide, H_2O_2 or NPS. Figure 5 shows oxidation by H_2O_2 and subsequent reduction with DTT (A), *Eco*Trx (B) or *Ptr*Trx (C) for the wild type enzyme. The kinetic analysis for reduction associated with recovery of activity could be performed using a model similar to that applied in oxidation (see Methods). While k″ values for DTT reduction were in the order of the unit ($M^{-1}\,s^{-1}$), Trxs reduced *Ptr*PGKase-1 with a second order rate constant of about 2000 $M^{-1}\,s^{-1}$ (Table 3 for wild type PGKase-1). In fact *Ptr*Trx reverted peroxide oxidation 3-fold faster than *Eco*Trx, but twice slower when reducing the diamide-oxidized enzyme (Table 3), indicating that *Ptr*PGKase-1 might be a potential target for diatom Trxs. All wild type and mutant enzymes displayed a single-step mechanism for reduction and similar kinetic constants (data not shown).

Redox Potentials of *Ptr*PGKase-1

As the activity of *Ptr*PGKase-1 could be reversibly modulated by redox modification, it was of interest to determine the midpoint potential of the wild type enzyme and its mutants by redox titration. We incubated fully reduced enzymes at various redox potentials, defined by variable amounts of 2-ME-HEDS at fixed 10 mM total concentration (at pH 8.0 and 25 °C). After 30 min incubation, enzymatic activity was measured. This time was sufficient to reach redox equilibrium between the enzyme and 2-ME. As expected, the maximal

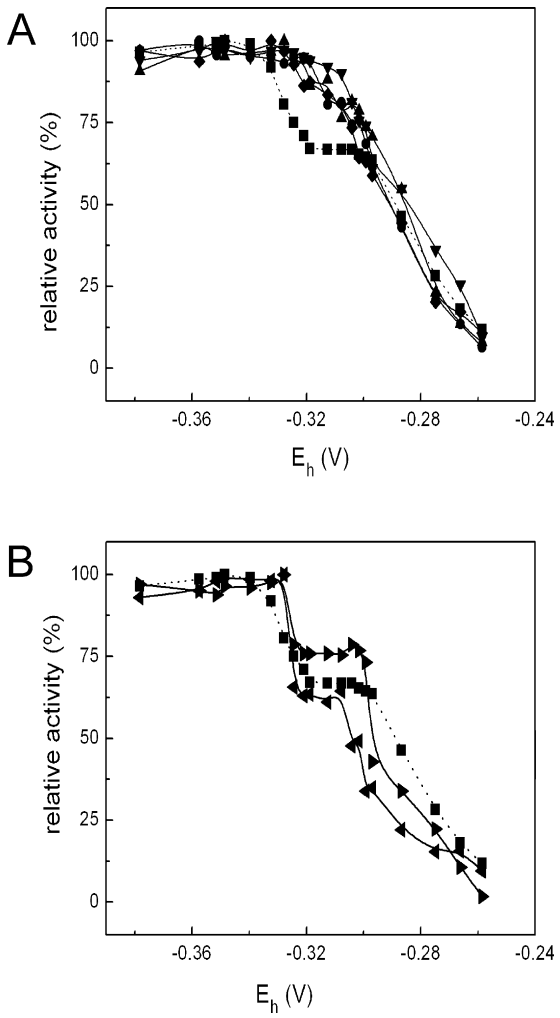

Figure 6. Redox titration of wild type and mutants *Ptr*PGKase-1. Enzymes (0.1 μM) were titrated at pH 8.0, at a total 2-ME-HEDS concentration of 10 mM, with a redox equilibration time of 30 min at 25 °C. Percentages of enzymatic activity, 100% being the maximum activity for each enzyme, were plotted as a function of E_h values. Wild type PGKase-1 (■, dotted line); (**A**) C21S (●), C58S (▲), C77S (▼), C95S (♦); (**B**) C214S (◄), C312S (►). Experimental data were fitted to Nernst equation for a two-electron redox system.

activity was achieved at the more negative E_h, consistent with the highest activity exhibited by the fully reduced enzyme (Fig. 6). We found that the curve for the wild type *Ptr*PGKase-1 curve was biphasic (Fig. 6A), resulting in the calculation of two E_m values (−0.329 ± 0.001 V and -0.282 ± 0.001 V) when fitted to the Nernst equation for a single-component, two-electron redox system to each part of the curve. This suggests the existence of more

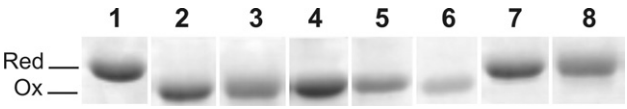

Figure 7. Non-reducing SDS-PAGE (8.5%) of oxidized and reduced wild type and mutant *Ptr*PGKase-1. Lanes: 1, reduced wild type *Ptr*PGKase-1; 2-8, oxidized enzymes (1 mM diamide at 25 °C for 20 min) as follows: 2, wild type enzyme; 3, C21S; 4, C58S; 5, C77S; 6, C95S; 7, C214S; 8, C312S.

than one redox center with differential characteristics in the enzyme. Both midpoint redox potentials fell within the range of values reported for other redox-active proteins (−0.280 to −0.330 V), including Trxs, ferredoxin-thioredoxin reductases and Trx regulated enzymes (Hicks et al. 2007; Hirasawa et al. 1999; Hutchison et al. 2000; Hutchison and Ort 1995). Thus, the data support the hypothesis that *Ptr*PGKase-1 could be sensitive to changes in the intracellular environment as is the case for plant proteins known to have important roles in redox-balancing systems.

As shown in Figure 6B, C214S and C312S mutant enzymes displayed the same biphasic behavior and equal E_m values than the wild type *Ptr*PGKase-1. To the contrary, mutations in Cys residues 21, 58, 77 and 95 implied the loss of the first E_m value (Fig. 6A), exhibiting only one redox potential as follows: C21S, −0.290 V; C58S, −0.287 V; C77S, −0.284 V; and C95S, −0.291 V. Parameters of inactivation kinetics and redox titration results suggest that C214 and C312 are poorly (or not at all) implicated in oxidative inactivation of the enzyme. On the other hand, loss of the more negative redox center observed after mutation of any of the remaining Cys residues suggests a 'collaborative' effect in the appearance of the first, thermodynamically more sensitive to oxidation, center.

Non-reducing PAGEs of Oxidized and Reduced *Ptr*PGKase-1

We examined if oxidation of *Ptr*PGKase-1 resulted in a change in mobility in non-reducing SDS-PAGE, as a consequence of, for example, oligomerization caused by disulphide bridge formation between Cys residues of different subunits. As shown in Figure 7 (lanes 1 and 2) no inter-subunit disulphide bridge was evident, since no molecular mass component related to oligomerization was observed; but modest shifts in the mobility of oxidized and reduced forms of the enzymes were detected. Oxidations carried out with 1 mM diamide and 0.5 mM H_2O_2

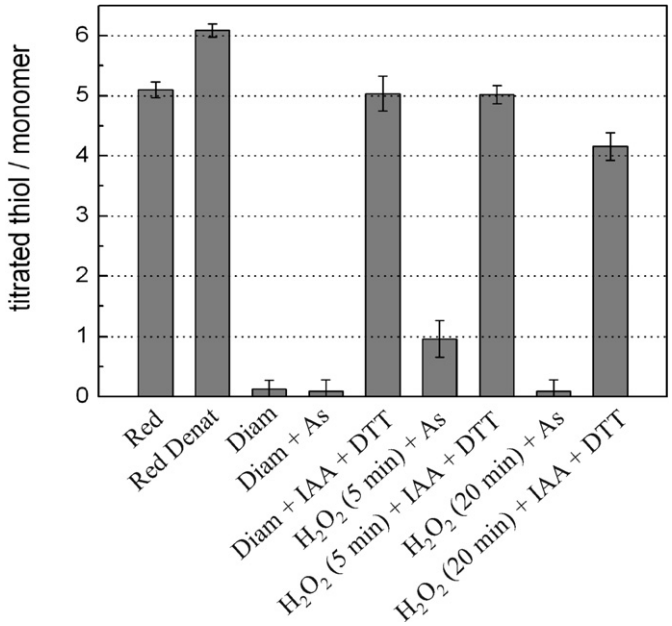

Figure 8. Quantification of thiols sensitive to oxidation and sulfenic acids in *Ptr*PGKase-1. Oxidation was carried out with 1 mM diamide ('Diam') for 20 minutes and 2 mM H_2O_2 during 5 min ['H_2O_2 (5 min)'] and 20 min ['H_2O_2 (20 min)'], enzyme concentration: 20 μM. Two different methods were applied from here: reduction with 10 mM arsenite for 60 min ('+ As'), or alkylation with 2 mM IAA (60 min) followed by reduction with 5 mM DTT for 20 min ('+ IAA + DTT'). Free thiols from both techniques were titrated with DTNB. A control without oxidant was also assayed with DTNB in its native ('Red') and denatured form ('Red Denat').

for 20 min resulted in a band ('Ox') with higher electrophoretic mobility than the 'Red' one, which was consistent with an intra-molecular disulphide bridge between two Cys residues distant in the protein primary sequence (Kang et al. 1999; Loferer et al. 1995). In both cases the oxidation was totally reversed by DTT and only the 'Red' band was observed.

All mutant enzymes displayed the same 'Red' band than the wild type *Ptr*PGKase-1 when incubated with reducing agents (data not shown). When oxidized, C21S, C58S, C77S and C95S mutant enzymes behaved identically to wild type *Ptr*PGKase-1 (Fig. 7, lanes 3-6). On the other hand, Figure 7 shows that mutants C214S and C312S (lanes 7 and 8) displayed different behavior from the wild type enzyme since the 'Ox' form of migration was not observed. We conclude that these two residues could be forming a disulphide bridge, but this seems not to be related with enzyme inactivation, as both mutants exhibited similar oxidation kinetics (Table 2) and patterns of oxidation-reduction potential than the wild type enzyme (Fig. 6). Results support the notion that the faster migration could be the consequence of the formation of a disulphide bridge between Cys-214 and Cys-312 in *Ptr*PGKase-1.

Sulfenic Acid and Disulphide Bridge Titration

In order to elucidate which residues were involved in the inactivation process and to infer the oxidation mechanism, chemical studies on Cys residues were carried out. DTNB (Ellman 1959) titration of the reduced wild type *Ptr*PGKase-1 showed that five Cys residues were accessible to the solvent or susceptible to the attack of oxidant agents in the native enzyme, while all of them were detected in the denatured enzyme (Fig. 8, 'Red' and 'Red Denat'). In order to quantify Cys residues sensitive to oxidation under different conditions, we incubated the *Ptr*PGKase-1 (20 μM) with 1 mM diamide during 20 min, washed it with dilution-concentration cycles to eliminate the excess of the oxidizing agent and then alkylated it with 2 mM IAA for 60 min at 25 °C. IAA is a Cys-alkylating agent that reacts with SH-groups. This covalent modification is not reverted by reductant agents (Zander et al. 1998). In this step only Cys remaining reduced during the first oxidative step were alkylated. After IAA incubation, the alkylating agent was washed out and 5 mM DTT was added to the enzyme, in order to reduce the oxidized, non-alkylated residues. Finally, the enzyme was washed again and thiols were quan-

tified with DTNB, after which only Cys residues oxidized in the first step could be detected. Results showed that five of the six Cys residues present in the wild type enzyme were able to be oxidized with diamide (Fig. 8, 'Diam + IAA + DTT'), which is coherent with the result explained in the previous paragraph. Hydrogen peroxide oxidation was also tested by incubation of 20 μM *Ptr*PGKase-1 with 2 mM H_2O_2 during two periods of time: 5 min and 20 min at 25 °C. In the first case, five thiols were detectable [Fig. 8, 'H_2O_2 (5 min) + IAA + DTT'] while, at the longer incubation, only four Cys were reducible by DTT [Fig. 8, 'H_2O_2 (20 min) + IAA + DTT'], consistent with one residue being over-oxidized and the other one being not susceptible to oxidation.

With the aim of recognizing sulfenic acids (-SOH), we oxidized *Ptr*PGKase-1 with 2 mM H_2O_2 during 5 min, washed the oxidizing agent out, and then quantified sulfenic acids using two methods: sodium arsenite reduction and NBD reaction. Sodium arsenite is a reducing agent specific for sulfenic acids (Radi et al. 1991; Saurin et al. 2004). When reducing the oxidized wild type enzyme with 10 mM arsenite followed by titration with DTNB, one thiol was detected, consistent with a stoichiometry of one –SOH per monomeric *Ptr*PGKase-1 [Fig. 8, 'H_2O_2 (5 min) + As']. When the incubation time with the oxidant agent was longer, no thiol was detected by this method [Fig. 8, 'H_2O_2 (20 min) + As'], probably because of over-oxidation of the sulfenic acid. Arsenite, as expected, did not revert the adduct formed between diamide and the Cys responsible for the sulfenic acid formation (Fig. 8, 'Diam + As'). Identification and stoichiometry of –SOH moieties were additionally verified using the reaction with NBD, as described by Ellis and Poole (Ellis and Poole 1997). A single -SOH was quantified at 347 nm in the oxidized enzyme but not in the reduced one (Fig. 9A). At 420 nm we quantified one thiol in the oxidized enzyme, which corresponded to the Cys residue refractory to oxidation. Results thus suggest that there are five cysteinyl residues susceptible to oxidation and one recalcitrant to be modified by oxidants. Of the former five residues, four are non-reducible with arsenite (thus, forming two disulphide bridges) and one that forms a sulfenic acid (that is then over-oxidized to sulfinic and sulfonic acid).

Chemical studies with PGKase-1 mutants are shown in Figure 9A and B. In order to detect sulfenic acid before over-oxidation occurred, analysis of the proper H_2O_2 concentration and incubation time were made. Finally, all oxidations were carried out with 0.5 mM H_2O_2 during 10 min. Figure 9C represents the final quantification of disulphide bridges and sulfenic acids for each mutant enzyme, calculated and deduced from Figure 9A and B. An evident disulphide bridge is formed between Cys-214 and 312, since the absence of any of them carried the loss of one disulphide bridge and the appearance of one more sulfenic acid. This bond would not be responsible for enzymatic activity loss but for the different electrophoretic mobility of the oxidized enzyme (Fig. 7).

From Figure 9 it can be concluded that Cys-77 is the residue forming the sulfenic acid. Also, the disappearance of a disulphide bond, along with the appearance of a second sulfenic acid in the mutant C58S, indicate that this residue is forming the second disulphide bond in the wild type enzyme. Then, from the two remaining Cys residues, Cys-21 and Cys-95, one should not be susceptible to oxidation, while the other should be responsible for the formation of a disulphide bridge with Cys-58. Mutant C21S shows similar results in thiol and sulfenic acid titration as the wild type enzyme (Fig. 9A and B); so, Cys-21 can be identified as the non-reducible residue. This is consistent with similar inactivation kinetics found for the wild type and the C21S mutant enzymes. Consequently the most probable candidate to form the disulphide bond with Cys-58 is Cys-95. When Cys-95 is absent, Cys-58 is oxidized to a highly reactive sulfenic acid, which afterward forms a disulphide bridge with the nearby Cys-21. This hypothesis is coherent with the titration of two disulphide bridges in this mutant (Fig. 9B) and the detection of Cys-21 in the denatured C95S enzyme (Fig. 9A and B). When Cys-58 is absent, Cys-95 would form a sulfenic acid (as seen in Fig. 9) and might be susceptible to over-oxidation.

Results in Figure 10 show the time dependence of irreversible inactivation for wild type and mutants *Ptr*PGKases-1 by hydrogen peroxide. Outcomes from Figure 10 gave support to previous arguments. C21S, C95S, C214S and C312S behaved similar to wild type PGKase-1, but C58S was irreversibly oxidized in a faster way. This is consistent with the loss of the second disulphide bridge and the appearance of a new sulfenic acid on Cys-95, obviously more susceptible to over-oxidation and important in enzymatic activity. C77S was less sensitive to irreversible inactivation, coherent with the fact that this residue is oxidized to sulfenic acid in wild type PGKase, with further over-oxidation to sulfinic and sulfonic acids. When Cys-77 is absent, the degree of irreversible oxidation is lower, as hydrogen peroxide attacks disulphide bridges slower than it does to unstable sulfenic acids.

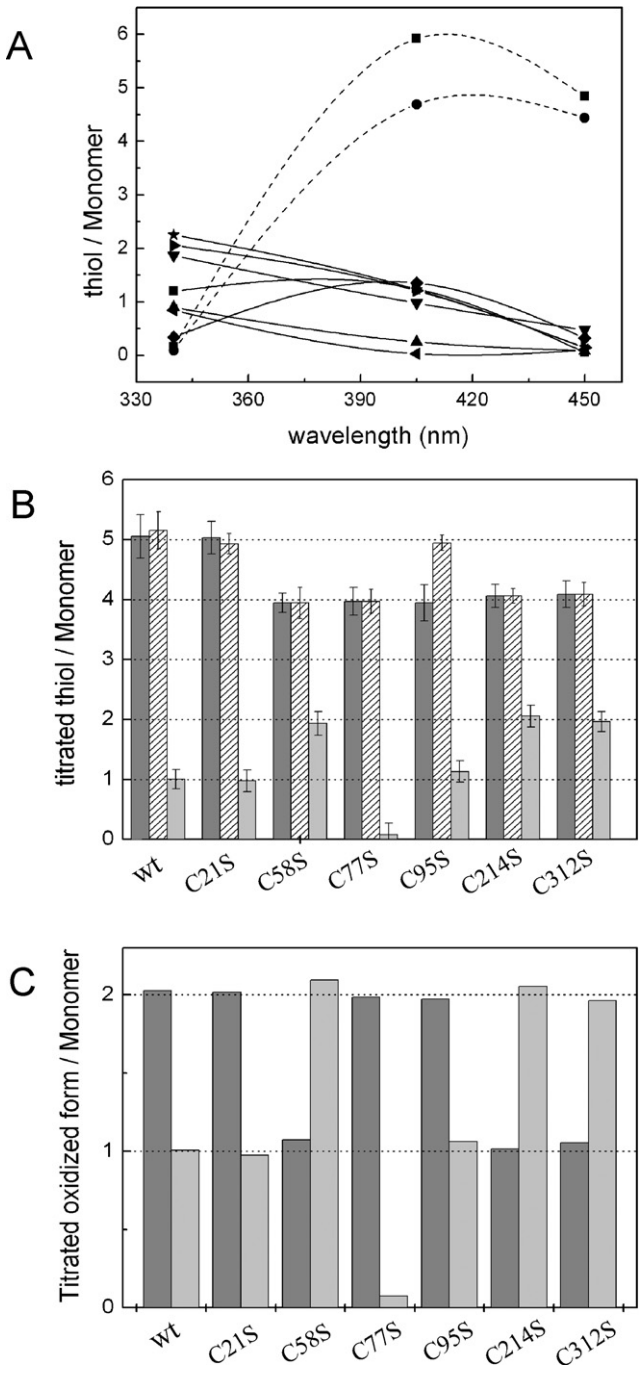

Figure 9. (**A**) Sulfenic acid quantification by change in NBD spectroscopic properties. 0.8 mM NBD reacted for 60 min with reduced (dash line) and oxidized (solid line) (0.5 mM H_2O_2, 10 min) wild type PGKase-1 (■) and mutants (all mutants exhibited identical behavior when reduced, •) (20 μM): C21S (▲), C58S (▼), C77S (♦), C95S (◄), C214S (►), C312S (⋆). (**B**) Quantification of thiols sensitive to oxidation and sulfenic acids in wild type *Ptr*PGKase-1 and mutants. Oxidation was carried out with 0.5 mM H_2O_2 during 10 min at 25 °C, enzyme concentration: 20 μM. Two alternative procedures were applied from here: 1) alkylation with 2 mM IAA (60 min) followed by reduction with 5 mM DTT, 20 min, with (lined bars) and without (dark gray bars) posterior denaturation of the enzyme (Cys susceptible to oxidation titration); and 2) reduction with arsenite (sulfenic acid and thiol not sensitive to oxidation quantification: light gray bars). Free remaining thiols from all procedures were quantified with DTNB. (**C**) Disulphide bridge quantity (dark gray bars) and sulfenic acid amount (light gray bars) present in oxidized wild type *Ptr*PGKase-1 and its Cys mutants, deduced from results in (**A**) and (**B**).

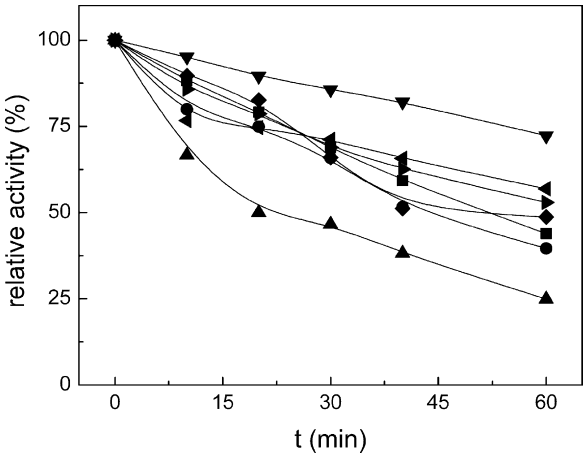

Figure 10. Time-dependent irreversible inactivation of wild type and mutants *Ptr*PGKase-1 by H_2O_2. Each enzyme (0.1 μM) was incubated with 1 mM H_2O_2 during the time indicated in the abscissa, with further reduction with 20 mM DTT for 15 min. Residual enzymatic activity was measured. Wild type PGKase-1 (■), C21S (•), C58S (▲), C77S (▼), C95S (♦), C214S (◄), C312S (►).

Discussion

Despite the importance of diatoms in biological sciences, there is scarce information about the characterization of enzymes from these organisms (Arias et al. 2010; Domergue et al. 2003; Michels et al. 2005). *P. tricornutum* is one of the most widely utilized model systems for studying the ecology, physiology, biochemistry and molecular biology of diatoms (Scala et al. 2002). However, the biochemical and physiological characterization of this microorganism is far from complete. A great advance to the understanding of its metabolism has been recently made with the elucidation of its entire genome (Bowler et al. 2008), so now it is necessary to characterize enzymes in order to address the

occurrence and functionality of metabolic scenarios in *P. tricornutum*.

We cloned, expressed and characterized the chloroplastidic PGKase-1 from *P. tricornutum*. It showed similar kinetic properties than the enzyme studied from other organisms, although the diatom enzyme displayed novel regulation characteristics. We found that *Ptr*PGKase-1 was susceptible to thiol-modifying agents in vitro, being active in its reduced form. It is concluded that the level of activity of the recombinant enzyme is determined by the redox state in the environment, which could have physiological relevance. The analysis of all the six Cys residues found in the diatom enzyme indicated that they have differences with respect to exposition and degree of reactivity toward thiol-modifying reagents. The enzyme displayed two values of midpoint redox potentials, consistent with the existence of two centers involved in redox regulation of enzymatic activity. Both potential values fell within the range of those reported for other redox-active proteins, including Trx-regulated enzymes from plants and green algae as spinach phosphoribulokinase (−290 mV), pea fructose-1,6-bis-phosphatase (-315 mV), spinach fructose-1,6-bis-phosphatase (-330 mV) and *Chlamydomonas reinhardtii* NADP-malate dehydrogenase (-280 mV) (Hirasawa et al. 1999; Lemaire et al. 2005). Thus, results support that *Ptr*PGKase-1 might be sensitive to changes in the intracellular redox environment (Hirasawa et al. 1999; Hutchison et al. 2000; Hutchison and Ort 1995). The lack of differences in E_m values in mutants C214S and C312S was not surprising, as the disulphide bridge that these two residues form is not involved in enzymatic activity loss. C21S, C58S, C77S and C95S mutant enzymes showed that any change in the 3PGA binding region lead to the loss of the more negative midpoint potential value, so all of them appear to contribute as a whole to that redox center. The oxidation-reduction kinetic constants obtained for wild type *Ptr*PGKase-1 were similar to those described for other in vivo redox regulated enzymes (Ballicora and Wolosiuk 1994; Geck and Hartman 2000).

Although no single mutant displayed insensitivity to inactivation by oxidation, Cys residues 58, 77 and 95 appear to be, all together, those responsible for loss of enzymatic activity. Our results support the notion that the oxidative mechanism leading to *Ptr*PGKase-1 inactivation is oxidation of Cys-77 to sulfenic acid and formation of a disulphide bond between Cys-58 and Cys-95. Cys-77 would be the first barrier to oxidant entrance, being in its oxidized form a sulfenic acid. Cys-21, Cys-77 and Cys-95 are located near residues essential for 3PGA binding (Asp-22, Asn-24, Arg-37, His-60, Arg-119). Oxidation of these three Cys residues may cause changes in their side chain sizes and/or electron densities that affect the positioning of neighboring residues, which alter binding of substrate and enzyme inhibition. The molecular model of *Ptr*PGKase-1 (see Fig. S2 A) details Cys residues positioned in the 3PGA binding site, with the residues important for substrate union painted in red. Cys-214 and Cys-312 form a disulphide bridge when oxidized [Fig. S2 (B)]. The latter would be responsible for differential electrophoretic mobility of oxidized *Ptr*PGKase-1, but not for enzymatic activity loss.

In general, there is scarce information about redox regulation of PGKases and no studies with physiological oxidant reagents were made. To our knowledge, the present work is the first one that describes this kind of extensive analysis of redox properties of PGKase. To have a closer view about how distinctive or general could be such a redox characteristic among PGKases, we constructed a phylogenetic tree including the enzyme from several organisms (Supplementary Fig. S3). To establish the phylogeny illustrated by Figure S3 we particularly analyzed cysteinyl residues contained in the amino acid sequences. It can be observed that *P. tricornutum* PGKase-1 is found within the same group of the chloroplastidic *T. pseudonana* enzyme. Both proteins have all of their 6 Cys residues conserved, after which it is tempting to speculate that the regulation herein described for the *P. tricornutum* enzyme might be a common mechanism of diatom chloroplastidic PGKases. On the other hand, it is observed in Figure S3 that the enzyme from diatoms is positioned near those from plants and green algae. Although PGKase had been identified as a Trx target in plants and algae (Balmer et al. 2004; Michelet et al. 2008; Rouhier et al. 2005), there is scarce information about the occurrence of specific redox mechanisms affecting the enzyme in these organisms. The spinach PGKase has two cysteinyl residues conserved with respect to Cys-95 and Cys-214 of *Ptr*PGKase-1, one of which was reported to be modified by DTNB with loss of activity (Kuntz and Krietsch 1982). While Cys-95 was found important for inhibition of the diatom enzyme, oxidation of Cys-214 caused no inactivation. Except for the enzyme from tobacco (*Nicotiana tabacum*), Cys-95 is conserved among PGKases from all eukaryotic organisms included in our analysis (Fig. S3). Also, plant enzymes possess Cys-214, except for wheat (*Triticum aestivum*), rice (*Oryza sativa*) and tobacco, as some algae too.

Thereby, Cys-95 appears as a possible candidate for regulation of the plant enzyme, as in diatoms; although the occurrence of such a redox mechanism in the former organisms is not clear enough with the current available information.

The group of PGKases reported to be inactivated by thiol-modifying agents is that including mammals and higher eukaryotes, for which two adjacent Cys residues located at the C-terminus are responsible (Huskins et al. 1982; Minard et al. 1989). This phylogenetic group is distant from *Ptr*PGKase-1 (Supplementary Fig. S3), so it is not surprising that the mechanism responsible for oxidation-inactivation is different. The fact of chloroplastidic diatom PGKases being similar to plant and algal enzymes but distinct from animal ones is coherent with the secondary endosymbiotic theory by which the diatom chloroplasts originated from a red alga with a primary chloroplast similar to the plant one (Scala et al. 2002). Apparently, oxidation of only one Cys would be enough for loss of activity in plants, although in diatoms there are 3 cysteinyl residues involved in inhibition. We do not know if this divergence is due to the losts of Cys in plants during evolution, after bifurcation, or if diatoms acquired cysteinyl residues important for regulation later. It is tempting to speculate that Cys multiplication in diatoms PGKase-1 might be functional for a finer regulation of enzymatic activity in chloroplasts, which may be involved in metabolic particularities observed for carbon partitioning in these microorganisms. Concerning the other two *P. tricornutum* PGKases, they are not significantly close to any phylogenetic group (Supplementary Fig. S3). PGKase-2 seems to be more related to thermophilic bacteria, while PGKase-51125 is further away from the described groups.

In plants, light-reduced thioredoxins activate several Calvin cycle enzymes, including fructose-1,6-bis-phosphatase, sedoheptulose-1,7-bis-phosphatase, RuBP carboxylase (RuBisCO) and glyceraldehyde-3-phosphate dehydrogenase (GAPDH) by reducing specific disulphide bridges or sulfenic acids to thiols [(Anderson 1986; Buchanan 1980); for review see (Buchanan 1991)]. Little is known about light regulation of diatom enzymes (if it occurs). A few reports analyzing some diatom photosynthetic enzymes show the lack of the Cys residues responsible for covalent redox regulation in their plant homologue proteins (Kroth et al. 2008; Michels et al. 2005; Ocheretina et al. 2000; Pancic and Strotmann 1993). Examples of the latter are the γ-subunit of the chloroplast ATPase (Pancic and Strotmann 1993) and malate dehydrogenase (Ocheretina et al. 2000). Also, diatom plastids possess a GAPDH, termed GapC1, that does not contain the cysteinyl residue responsible for redox regulation, so it was reported that it would not be affected by oxidation or reduction (Kroth et al. 2008; Michels et al. 2005). Phosphoribulokinase activity is redox regulated in vitro, but its midpoint potential revealed that under cellular redox conditions the diatom enzyme is generally active and might not be regulated by thioredoxin (Michels et al. 2005). The plastidic fructose-bis-phosphatase is the only enzyme in diatoms for which there is direct evidence of redox-regulation by thioredoxin (Michels et al. 2005).

It has been described that no tight regulation of the Calvin cycle in *P. tricornutum* would be necessary because of the absence of a complete OPP in the chloroplast, so some previous work indicated that Trx could not play a role in light regulation of plastidic enzymes from this organism (Kroth et al. 2008; Ocheretina et al. 2000). Results obtained in this work suggest that *Ptr*PGKase-1 is a potential target for diatom physiological oxidizing agents and Trxs, and could be redox-regulated in vivo. On the other hand, it was also described that all enzymes involved in glycolysis are present in diatom plastids, so this pathway might be active in chloroplasts (Kroth et al. 2008) and tight regulation of glycolysis and Calvin cycle would be necessary for preventing futile cycles. Since only one plastidic isoenzyme of PGKase was identified and because of the principle of microscopic reversibility, *Ptr*PGKase-1 would not be responsible for regulating both metabolic pathways in order to avoid glycolysis and Calvin cycle to act simultaneously.

PGKase had been identified as a Trx target in plants, algae and mammals (Balmer et al. 2004; Fernando et al. 1992; Michelet et al. 2008; Rouhier et al. 2005) and as a site of S-thiolation in algae and mammals (Fratelli et al. 2002; Michelet et al. 2008), when exposed to oxidant agents. These previous reports proposed that glutathionylation and oxidation could affect PGKase activity under oxidative stress conditions. Concerning redox regulation of PGKase-1 in *P. tricornutum*, it could function as a sensor of the redox state environment, which could track triose-phosphate to metabolic pathways responsible for producing reducing power as NADPH (for example OPP). The latter could be used to minimize ROS formation and to repair damages caused by oxidative stress via the thioredoxin and glutathione systems, known to be active in *P. tricornutum* (Arias et al. 2010).

Methods

Materials: Bacteriological media components were from Britania Laboratories (Rosario, Santa Fe, Argentina). Enzymes for molecular biology protocols were from Promega (Madison, WI, USA). NADH, ATP, 3PGA, diamide, NPS, DTT, NBD, IAA were purchased from Sigma-Aldrich (St. Louis, MO, USA). All other chemicals were of the highest quality commercially available.

Strains and plasmids: *Phaeodactylum tricornutum*, strain LFF Pt 01 from Laboratorio de Fermentaciones, FBCB, UNL (strain available upon request, e-mail: abeccari@fbcb.unl.edu.ar), was grown as described by Arias (Arias et al. 2010). *Escherichia coli* TOP 10 (Invitrogen) cells and *Escherichia coli* Rosetta (DE3) were utilized in routine plasmid construction and expression experiments, respectively. The vector pGEM-T Easy (Promega) was used for cloning and sequencing purposes. The expression vector was pET-19b (Novagen). The [pRSET-A/*Ptr*Trx-h2] plasmid for expression of *Ptr*Trx was kindly provided by Dr. Diego Arias (unpublished results). DNA manipulation, *E. coli* culture and transformation were performed according to standard protocols (Maniatis et al., 1982).

RNA extraction, RT-PCR and cloning: Total RNA from *P. tricornutum* was isolated as previously described (Domergue et al. 2002). cDNA was synthesized at 42 °C for 1 h in a 25 μl reaction mixture containing 0.25 μg RNA, 200 pmol oligo(dT) primer and 200 U of M-MLV reverse transcriptase (USB, Cleveland, OH, USA). The oligonucleotide primer pair (FwPGK1*Ptr* and RvPGK1*Ptr*, Table S2) utilized for PCR amplification of the gene encoding PGKase-1 (*Ptr*PGKase-1) was designed from the sequence available in the NCBI database (AF108451). The PCR reaction was performed in a 50 μl reaction mixture containing 2 μl cDNA solution, 100 pmol of each primer, 10 pmol of each dNTP and 2.5 U *Taq* DNA polymerase (Fermentas). The protocol for PCR amplification was: 95 °C for 5 min; 57 °C for 1 min; 72 °C for 10 min; 30 cycles of 95 °C for 1 min, 57 °C for 0.5 min, and 72 °C for 2.5 min; then 72 °C for 10 min. The PCR product was purified and ligated into the pGEM-T Easy vector (Promega). Correctness of the amplified gene was confirmed on both strands by complete DNA sequencing (Macrogen, Seoul, Korea). Sequences were analyzed using Vector NTI Advance 10 (Invitrogen) program. The cloned plasmid was digested and the gene was ligated to the expression vector pET-19b (Novagen) to obtain the recombinant protein fused to a His_{10}-tag in the N-term.

Construction of *Ptr*PGKase-1 mutants: Site-specific mutants C21S, C58S, C77S, C95S, C214S and C312S were constructed according to the procedures of the QuickChange Site-Directed Mutagenesis kit (Stratagene), using the above described pET-19b/PGKase-1 constructed as template and the primers described in Table S2. The QuickChange reaction was performed in a 50 μl reaction mixture containing 1 μl template solution, 125 pg of each primer, 10 pmol of each dNTP and 2.5 U *Pfu* DNA polymerase (Fermentas). The protocol for PCR amplification was: 95 °C for 0.5 min; 12 cycles of 95 °C for 1 min, 55 °C for 1 min, and 72 °C for 14 min. *Dpn*I digestion was carried out three times with 10 μl QuickChange product, 10 U *Dpn*I, for 2 h at 37 °C. All genes were fully sequenced to verify that only the desired mutation was generated.

Heterologous expression and protein purification: Competent *E. coli* Rosetta (DE3) cells were transformed with the above described expression vectors (for wild type and mutant enzymes) and cultured in LB medium supplemented with 100 μg ml^{-1} ampicillin at 37 °C, under shaking at 200 rpm. Overnight cultures were 1/100 diluted in fresh LB medium supplemented with 100 μg ml^{-1} ampicillin and grown up to $OD_{600} \sim 0.6$. The expression was induced at 25 °C, for 16 h with 0.2 mM IPTG, after which cells were harvested by centrifugation. All purification of *Ptr*PGKase-1 (wild type and mutant forms), and *Ptr*Trx were conducted at 0 °C to 4 °C. Cells were resuspended in buffer A [25 mM Tris-HCl, pH 8.0, 0.1 mM EDTA, 1 mM, 0.3 M NaCl, 5% glycerol], disrupted by sonication and the lysate clarified by centrifugation. All recombinant enzymes were purified by the same procedure. The resultant crude extract was loaded in a Sepharose-IDA-Ni^{2+} column. The column was washed with buffer A (alone and plus the addition of and 35 mM imidazole), and then eluted with 300 mM imidazole in buffer A. Fractions containing PGKase activity were pooled, incubated with 10 mM 2-ME for 30 min, desalted in buffer B (25 mM Tris-HCl, pH 8.0, 0.1 mM EDTA, 0.3 M NaCl, 10% glycerol) and stored at −80 °C. When purifying *Ptr*Trx, fractions containing this protein were pooled, supplemented with 10% glycerol and stored at −80 °C. Under the specified conditions, recombinant enzymes were stable for, at least, one year.

Enzymatic activity: All enzyme assays were performed in a Multiskan scent one-channel vertical light path filter photometer (Thermo Electron Co.), at 30 °C and a final volume of 50 μl. One unit (U) of activity is defined as the amount of enzyme catalyzing the production of 1 μmol of product per minute, at 30 °C, under the specified assay conditions. Unless otherwise indicated, enzyme activity was determined measuring the reaction of 3PGA phosphorylation to 1,3-bis-phospho-glycerate coupled to the reaction of the NAD-dependent GAPDH, as described by Bücher (Bücher 1955). Consumption of NADH was followed measuring absorbance at 340 nm in a reaction mixture containing 50 mM Tris-HCl, pH 8.0, 5 mM ATP, 5 mM 3PGA, 5 mM $MgCl_2$, 0.2 mM NADH, 1 U ml^{-1} GAPDH (Sigma), plus a suitable amount of PGKase-1.

Protein methods: Reducing SDS-PAGE was carried out using the Bio-Rad minigel equipment, according to previously described methods (Laemmli 1970). Non-reducing SDS-PAGE was carried out without the addition of 2-ME in the sample buffer. Coomasie Brillant Blue was used to stain protein bands. Protein concentration was determined by the method of (Bradford 1976) using BSA as standard.

Gel filtration on a Superdex 200 Prep Grade (Amersham Pharmacia Biotech) column was conducted to determine the native molecular mass of *Ptr*PGKase-1. The column was equilibrated with 25 mM Tris-HCl, pH 8.0, 100 mM NaCl and 0.1 mM EDTA, and calibrated with the molecular mass markers: carbonic anhydrase (30 kDa), ovalbumin (43 kDa), BSA (67 kDa) and horse IgG (140 kDa).

Oxidation and reduction kinetic studies: Oxidative treatments were performed at 25 °C by incubation of 0.1 μM wild type and mutant enzymes (E) with molar excess of oxidant agents (I): 0 to 1 mM diamide, 0 to 10 mM hydrogen peroxide, 0 to 5 mM oxidized glutathione (GSSG) or 0 to10 mM sodium nitroprusside (NPS), at variable times, in buffer B. At different incubation times, a 10 μl aliquot was tested for remaining enzymatic activity. Plots of percentages of residual enzyme activity [relative activity (%)] (on a log scale) versus time (t, lineal scale) were fitted to: log relative activity = 2 − k′obs t equation. The plot of k'_{obs} values vs. variable oxidant concentrations was consistent with the two-step mechanism irreversible inhibition (Copeland 2005):

$$E + I \overset{K_I}{\rightleftarrows} EI \xrightarrow{k'} E\text{-}I \quad k'_{obs} = \frac{k' \times I}{K_I + I} \quad k'' = \frac{k'}{K_I}$$

For this mechanism, k′ defines the maximum rate of inactivation that is achieved at infinite concentration of inactivator, K_I describes the concentration of inhibitor yielding a rate of

inactivation equal to half k′, and $k'' = k' / K_I$ is the second-order rate, which is considered to be the best measure of relative inactivator potency or effectiveness.

Reduction experiments were performed with 0.1 μM oxidized enzyme, by incubation with DTT, *E. coli* Trx (*Eco*Trx) or *Ptr*Trx. *Ptr*PGKase-1 was incubated with 0.5 mM H_2O_2 (20 min), 0.25 mM diamide (30 min) or 2 mM NPS (40 min) at 25 °C, diluted to eliminate the excess of oxidizing reagent and then incubated at variable times with different concentrations of reducing agents: 0 to 10 mM DTT, 0 to 10 μM *Eco*Trx or 0 to 3.5 μM *Ptr*Trx. At each incubation time, a 10 μl aliquot was tested for enzyme activity. k'_{obs} for each activator was obtained as explained for oxidative treatments and obtained k'_{obs} values were plotted against variable reducing agent concentrations and a linear fit was used, coherent with a single-step mechanism ($k'_{obs} = k''$ [Red]) (Copeland 2005). All graphs and data fittings were made using the program Origin 7.0 (OriginLab Corporation).

Determination of redox potentials: The dependence of *Ptr*PGKase-1 activity on redox potential was examined using redox buffers containing defined ratios of reduced and oxidized 2-ME [2-ME and hydroxyethyldisulphide (HEDS), respectively] (Hutchison and Ort 1995). Protein samples (0.1 μM) were equilibrated in media containing 25 mM Tris-HCl pH 8.0 and 10 mM total 2-ME/HEDS for 30 min at 25 °C. After equilibration, aliquots were withdrawn and assayed for enzyme activity. E_h values were determined by using the Nernst equation:

$$E_h = E_{m,pH\ 8.0} + RT/nF \ln([Ox]/[Red]),$$

being RT/F = 0.0257 V, n = 2, and $E_{m,\ pH\ 8.0}$ −0.319 V for 2-ME (Lees and Whitesides 1993). Data were also fitted to the Nernst equation for a single-component two-electron redox system, in order to obtain ethe corresponding $E_{m,\ pH\ 8.0}$ value.

Chemical characterization and quantification of redox modifications: Modifications of sulfenic acid- and thiol-containing proteins were performed under anaerobic conditions, using degasified buffers and water. Sulfhydryls were quantified using DTNB at 412 nm (extinction coefficient = 13,600 M^{-1} cm^{-1}) (Ellman 1959). Reduced or oxidized proteins, in their native or denatured forms (urea 6 M), were incubated with 2 mM DTNB for 30 min at 30 °C in the dark and absorbance at 412 nm was measured. Sulfenic acids were quantified by reduction of oxidized enzymes with the SOH-specific reducing agent sodium arsenite (Radi et al. 1991; Saurin et al. 2004). Enzymes (20 μM) were reversibly oxidized with 2 mM H_2O_2 for 5 min, the oxidant removed by dilution-concentration cycles, using Microcom columns (Millipore), and then incubated with 10 mM sodium arsenite during 60 min at 25 °C. Reduced thiols were quantified with DTNB as described above.

The identity of sulfenic acids was further confirmed by the 7-chloro-4-nitrobenzo-2-oxa-1, 3, diazole (NBD) assay, as described by Ellis and Poole (Ellis and Poole 1997), measuring absorbance at 420 nm and 347 nm for NBD adducts with thiols and sulfenic acids in proteins, respectively. An extinction coefficient of 13,400 M^{-1} cm^{-1} (at both wavelengths) was used to quantify the NBD-thiol or NBD-sulfenic acid product (Ellis and Poole 1997). Reduced or oxidized enzymes (20 μM) were mixed with a small volume on NBD in dimethyl sulfoxide (final concentration = 0.8 mM) and incubated for 30 min at 25 °C in the dark. Final spectra were taken after free NBD was removed by four concentration-dilution cycles with buffer B in an ultrafiltration device. Alquilation of thiols was carried out incubating enzymes (20 μM) with 2 mM iodoacetic acid (IAA) in the dark for 60 min at 25 °C (Zander et al. 1998).

Homology modeling: A 3D model of the open conformation of *Ptr*PGKase-1 was built using the program Modeller 9v2 (Sali and Blundell 1993), employing as templates known coordinates of PGKase form pig (*Sus scrofa*) muscle (PDB ID: 1VJC) and from *Thermus caldophilus* (PDB ID: 2IE8), available at the Protein Data Bank server http://www.rcsb.org/pdb/home/home.do, both displaying 44.4% of homology with *Ptr*PGKase-1. Sequence alignment was performed with BioEdit 7.0.9.0 software http://www.mbio.ncsu.edu/BioEdit/BioEdit.html and accuracies of the models were checked using the Verify-3D server http://nihserver.mbi.ucla.edu/Verify_3D. Model illustrations and distance calculations were made with VMD software http://www.ks.uiuc.edu.

Phylogenetic methods: PGKase sequences were aligned using BioEdit 7.0.9.0 software. Phylogenetic analyses were conducted using PHYLIP v. 3.67 (Felsenstein 1989), employing the PROTDIST program and the Jones-Taylor-Thornton (JTT) model for distance matrix calculation, and Fitch-Margoliash as the tree drawing method (Kitsch program).

Acknowledgements

This work was supported by grants from ANPCyT (PICT'08 No. 1754), CONICET (PIP 2519), and UNL (CAI+D Redes & Orientado). MBB is a doctoral fellow from CONICET and AAI is a principal investigator from the same institution. The authors thank Dr. Alejandro Beccaria and Dr. Diego Arias for useful technical advices, and for kindly provide diatom cells (AB) and the plasmid for expression of thioredoxin from *P. tricornutum* (DA).

Appendix A. Supplementary data

Supplementary data associated with this article can be found, in the online version, at doi:10.1016/j.protis.2011.07.001.

References

Anderson LE (1986) Light/dark Modulation of Enzyme Activity in Plants. In Kader J-C, Delseny M (eds) Advances in Botanical Research **Vol 12**. Academic Press, New York, pp 1–46

Arias DG, Marquez VE, Beccaria AJ, Guerrero SA, Iglesias AA (2010) Purification and characterization of a glutathione reductase from *Phaeodactylum tricornutum*. Protist **161**:91–101

Balmer Y, Koller A, Val GD, Schürmann P, Buchanan BB (2004) Proteomics uncovers proteins interacting electrostatically with thioredoxin in chloroplasts. Photosynth Res **79**:275–280

Ballicora MA, Wolosiuk RA (1994) Enhancement of the reductive activation of chloroplast fructose-1,6-bisphosphatase by modulators and protein perturbants. Eur J Biochem **222**:467–474

Banks RD, Blake CC, Evans PR, Haser R, Rice DW, Hardy GW, Merrett M, Phillips AW (1979) Sequence, structure and

activity of phosphoglycerate kinase: a possible hinge-bending enzyme. Nature **279**:773–777

Bowler C, Allen AE, Badger JH, Grimwood J, Jabbari K, Kuo A, Maheswari U, Martens C, Maumus F, Otillar RP, Rayko E, Salamov A, Vandepoele K, Beszteri B, Gruber A, Heijde M, Katinka M, Mock T, Valentin K, Verret F, Berges JA, Brownlee C, Cadoret JP, Chiovitti A, Choi CJ, Coesel S, De Martino A, Detter JC, Durkin C, Falciatore A, Fournet J, Haruta M, Huysman MJ, Jenkins BD, Jiroutova K, Jorgensen RE, Joubert Y, Kaplan A, Kroger N, Kroth PG, La Roche J, Lindquist E, Lommer M, Martin-Jezequel V, Lopez PJ, Lucas S, Mangogna M, McGinnis K, Medlin LK, Montsant A, Oudot-Le Secq MP, Napoli C, Obornik M, Parker MS, Petit JL, Porcel BM, Poulsen N, Robison M, Rychlewski L, Rynearson TA, Schmutz J, Shapiro H, Siaut M, Stanley M, Sussman MR, Taylor AR, Vardi A, von Dassow P, Vyverman W, Willis A, Wyrwicz LS, Rokhsar DS, Weissenbach J, Armbrust EV, Green BR, Van de Peer Y, Grigoriev IV (2008) The *Phaeodactylum* genome reveals the evolutionary history of diatom genomes. Nature **456**:239–244

Bradford MM (1976) A rapid and sensitive method for the quantitation of microgram quantities of protein utilizing the principle of protein-dye binding. Anal Biochem **72**:248–254

Buchanan BB (1980) Role of light in the regulation of chloroplast enzymes. Annu Rev Plant Physiol **288**:1–9

Buchanan BB (1991) Regulation of CO2 assimilation in oxygenic photosynthesis: the ferredoxin/thioredoxin system. Perspective on its discovery, present status, and future development. Arch Biochem Biophys **288**:1–9

Bücher T (1955) Phosphoglycerate kinase from Brewer's yeast. Methods Enzymol **1**:415–422

Copeland RA (2005) Evaluation of enzyme inhibitors in drug discovery. A guide for medicinal chemists and pharmacologists. Methods Biochem Anal **46**:1–265

Cserpan I, Vas M (1983) Effects of substrates on the heat stability and on the reactivities of thiol groups of 3-phosphoglycerate kinase. Eur J Biochem **131**:157–162

Dekany K, Vas M (1984) Inactivation of pig muscle 3-phosphoglycerate kinase by thiol modification depends on reagent size. Eur J Biochem **139**:125–130

Domergue F, Lerchl J, Zahringer U, Heinz E (2002) Cloning and functional characterization of *Phaeodactylum tricornutum* front-end desaturases involved in eicosapentaenoic acid biosynthesis. Eur J Biochem **269**:4105–4113

Domergue F, Spiekermann P, Lerchl J, Beckmann C, Kilian O, Kroth PG, Boland W, Zahringer U, Heinz E (2003) New insight into *Phaeodactylum tricornutum* fatty acid metabolism. Cloning and functional characterization of plastidial and microsomal delta12-fatty acid desaturases. Plant Physiol **131**:1648–1660

Ellis HR, Poole LB (1997) Novel application of 7-chloro-4-nitrobenzo-2-oxa-1,3-diazole to identify cysteine sulfenic acid in the AhpC component of alkyl hydroperoxide reductase. Biochemistry **36**:15013–15018

Ellman GL (1959) Tissue sulfhydryl groups. Arch Biochem Biophys **82**:70–77

Felsenstein J (1989) PHYLIP: phylogeny inference package (version 3.2). Cladistics **5**:164–166

Fernando MR, Nanri H, Yoshitake S, Nagata-Kuno K, Minakami S (1992) Thioredoxin regenerates proteins inactivated by oxidative stress in endothelial cells. Eur J Biochem **209**:917–922

Fifis T, Scopes RK (1978) Purification of 3-phosphoglycerate kinase from diverse sources by affinity elution chromatography. Biochem J **175**:311–319

Fratelli M, Demol H, Puype M, Casagrande S, Eberini I, Salmona M, Bonetto V, Mengozzi M, Duffieux F, Miclet E, Bachi A, Vandekerckhove J, Gianazza E, Ghezzi P (2002) Identification by redox proteomics of glutathionylated proteins in oxidatively stressed human T lymphocytes. Proc Natl Acad Sci USA **99**:3505–3510

Fritz PJ, White EL (1974) 3-Phosphoglycerate kinase from rat tissues. Further characterization and developmental studies. Biochemistry **13**:444–449

Geck MK, Hartman FC (2000) Kinetic and mutational analyses of the regulation of phosphoribulokinase by thioredoxins. J Biol Chem **275**:18034–18039

Gruber A, Weber T, Bartulos CR, Vugrinec S, Kroth PG (2009) Intracellular distribution of the reductive and oxidative pentose phosphate pathways in two diatoms. J Basic Microbiol **49**:58–72

Hicks LM, Cahoon RE, Bonner ER, Rivard RS, Sheffield J, Jez JM (2007) Thiol-based regulation of redox-active glutamate-cysteine ligase from *Arabidopsis thaliana*. Plant Cell **19**:2653–2661

Hirasawa M, Schurmann P, Jacquot JP, Manieri W, Jacquot P, Keryer E, Hartman FC, Knaff DB (1999) Oxidation-reduction properties of chloroplast thioredoxins, ferredoxin:thioredoxin reductase, and thioredoxin f-regulated enzymes. Biochemistry **38**:5200–5205

Huskins KR, Bernhard SA, Dahlquist FW (1982) Halibut muscle 3-phosphoglycerate kinase. Chemical and physical properties of the enzyme and its substrate complexes. Biochemistry **21**:4180–4188

Hutchison RS, Ort DR (1995) Measurement of equilibrium midpoint potentials of thiol/disulfide regulatory groups on thioredoxin-activated chloroplast enzymes. Methods Enzymol **252**:220–228

Hutchison RS, Groom Q, Ort DR (2000) Differential effects of chilling-induced photooxidation on the redox regulation of photosynthetic enzymes. Biochemistry **39**:6679–6688

Joao HC, Williams RJ (1993) The anatomy of a kinase and the control of phosphate transfer. Eur J Biochem **216**:1–18

Kang JG, Paget MS, Seok YJ, Hahn MY, Bae JB, Hahn JS, Kleanthous C, Buttner MJ, Roe JH (1999) RsrA, an anti-sigma factor regulated by redox change. EMBO J **18**:4292–4298

Krietsch WK, Bucher T (1970) 3-phosphoglycerate kinase from rabbit sceletal muscle and yeast. Eur J Biochem **17**:568–580

Krietsch WK, Eber SW, Haas B, Ruppelt W, Kuntz GW (1980) Characterization of a phosphoglycerate kinase deficiency variants not associated with hemolytic anemia. Am J Hum Genet **32**:364–373

Kroth PG, Chiovitti A, Gruber A, Martin-Jezequel V, Mock T, Parker MS, Stanley MS, Kaplan A, Caron L, Weber T,

Maheswari U, Armbrust EV, Bowler C (2008) A model for carbohydrate metabolism in the diatom *Phaeodactylum tricornutum* deduced from comparative whole genome analysis. PLoS ONE **3**:e1426

Kuntz GW, Krietsch WK (1982) Phosphoglycerate kinase from spinach, blue-green algae, and yeast. Methods Enzymol **90 Pt E**:110–114

Laemmli UK (1970) Cleavage of structural proteins during the assembly of the head of bacteriophage T4. Nature **227**:680–685

Larsson-Raznikiewicz M, Arvidsson L (1971) Inhibition of phosphoglycerate kinase by products and product homologues. Eur J Biochem **22**:506–512

Lees WJ, Whitesides GM (1993) Equilibrium constants for thiol-disulfide interchange reactions: A coherent, corrected set. J Org Chem **58**:642–647

Lemaire SD, Quesada A, Merchan F, Corral JM, Igeno MI, Keryer E, Issakidis-Bourguet E, Hirasawa M, Knaff DB, Miginiac-Maslow M (2005) NADP-malate dehydrogenase from unicellular green alga *Chlamydomonas reinhardtii*. A first step toward redox regulation? Plant Physiol **137**:514–521

Liaud MF, Lichtlé C, Apt K, Martin W, Cerff R (2000) Compartment-specific isoforms of TPI and GAPDH are imported into diatom mitochondria as a fusion protein: evidence in favor of a mitochondrial origin of the eukaryotic glycolytic pathway. Mol Biol Evol **17**:213–223

Loferer H, Wunderlich M, Hennecke H, Glockshuber R (1995) A bacterial thioredoxin-like protein that is exposed to the periplasm has redox properties comparable with those of cytoplasmic thioredoxins. J Biol Chem **270**:26178–26183

Maniatis TF, Fritsch EF, Sambrook J (1982) Molecular Cloning: A Laboratory Manual. Cold Spring Harbor Laboratory, New York

Markland FS, Bacharach AD, Weber BH, O'Grady TC, Saunders GC, Umemura N (1975) Chemical modification of yeast 3-phosphoglycerate kinase. J Biol Chem **250**:1301–1310

Michelet L, Zaffagnini M, Vanacker H, Le Marechal P, Marchand C, Schroda M, Lemaire SD, Decottignies P (2008) In vivo targets of S-thiolation in *Chlamydomonas reinhardtii*. J Biol Chem **283**:21571–21578

Michels AK, Wedel N, Kroth PG (2005) Diatom plastids possess a phosphoribulokinase with an altered regulation and no oxidative pentose phosphate pathway. Plant Physiol **137**:911–920

Mildvan AS, Leigh RA (1964) Determination of co-factor dissociation constants from the kinetics of inhibition of enzymes. Biochim Biophys Acta **89**:393–397

Minard P, Desmadril M, Ballery N, Perahia D, Mouawad L, Hall L, Yon JM (1989) Study of the fast-reacting cysteines in phosphoglycerate kinase using chemical modification and site-directed mutagenesis. Eur J Biochem **185**:419–423

Nojima H, Oshima T, Noda H (1979) Purification and properties of phosphoglycerate kinase from *Thermus thermophilus* strain HB8. J Biochem **85**:1509–1517

Ocheretina O, Haferkamp I, Tellioglu H, Scheibe R (2000) Light-modulated NADP-malate dehydrogenases from mossfern and green algae: insights into evolution of the enzyme's regulation. Gene **258**:147–154

Pancic PG, Strotmann H (1993) Structure of the nuclear encoded gamma subunit of CF0CF1 of the diatom *Odontella sinensis* including its presequence. FEBS Lett **320**:61–66

Pawluk A, Scopes RK, Griffiths-Smith K (1986) Isolation and properties of the glycolytic enzymes from *Zymomonas mobilis*. The five enzymes from glyceraldehyde-3-phosphate dehydrogenase through to pyruvate kinase. Biochem J **238**:275–281

Radi R, Beckman JS, Bush KM, Freeman BA (1991) Peroxynitrite oxidation of sulfhydryls. The cytotoxic potential of superoxide and nitric oxide. J Biol Chem **266**:4244–4250

Rouhier N, Villarejo A, Srivastava M, Gelhaye E, Keech O, Droux M, Finkemeier I, Samuelsson G, Dietz KJ, Jacquot JP, Wingsle G (2005) Identification of plant glutaredoxin targets. Antioxid Redox Signal **7**:919–929

Sali A, Blundell TL (1993) Comparative protein modelling by satisfaction of spatial restraints. J Mol Biol **234**:779–815

Saurin AT, Neubert H, Brennan JP, Eaton P (2004) Widespread sulfenic acid formation in tissues in response to hydrogen peroxide. Proc Natl Acad Sci USA **101**:17982–17987

Scala S, Carels N, Falciatore A, Chiusano ML, Bowler C (2002) Genome properties of the diatom *Phaeodactylum tricornutum*. Plant Physiol **129**:993–1002

Zander T, Phadke ND, Bardwell JC (1998) Disulfide bond catalysts in *Escherichia coli*. Methods Enzymol **290**:59–74

Zomer AW, Allert S, Chevalier N, Callens M, Opperdoes FR, Michels PA (1998) Purification and characterisation of the phosphoglycerate kinase isoenzymes of *Trypanosoma brucei* expressed in *Escherichia coli*. Biochim Biophys Acta **1386**:179–188